Table IV. Solvent Exchange Rate Constants (10^7 s^{-1}) at 298.15 K for Water and DMF on Heavy Lanthanide Ions

metal ion	Tb^{3+}	Dy^{3+}	Ho^{3+}	Er^{3+}	Tm^{3+}	Yb^{3+}
ionic radius[a]	109.5	108.3	107.2	106.2	105.2	104.2
rate constant $Ln(H_2O)_9{}^{3+}$	49.6	38.6	19.1	11.8	8.1	4.1
rate constant $Ln(DMF)_8{}^{3+}$ [b]	1.9	0.63	0.36	1.3	3.1	9.9
exchange mechanism	I_d	I_d	I_d	I_d, D	D	D

[a] In pm, taken from ref 45 for CN = 9. [b] From ref 11.

series of heavy lanthanides, following the trend in ionic radii. The water exchange rate constants are very close to the substitution rate of water by sulfate (5.2×10^8 s^{-1} for Tb^{3+} to 0.8×10^8 s^{-1} for Yb^{3+}), determined by ultrasonic absorption.[41] These substituion rates increase from La^{3+} to Sm^{3+} and decrease from Eu^{3+} to Lu^{3+}. Unfortunately, it is impossible to say whether the water exchange rate will follow the same trend, or whether it will continue to increase with the increase of ionic radii for the lighter elements.[42] However, a lower limit value of 10^9 s^{-1} has been determined for the exchange on Nd^{3+} (5.2×10^8 s^{-1} for the sulfate complexation[41]). This tends to indicate that the aqua ions at the beginning of the series are more labile than those at the end.

If water exchange on the aqua ions is very fast, the exchange process will be diffusion-controlled,[43] and it is debatable whether or not a kinetically distinguishable first coordination sphere still exists for such labile species. For the heavy lanthanide ions, the exchange rate is more than 180 times slower (for Gd^{3+}) than the diffusion rate, and it still makes a sense to use the model of an ion surrounded by a well-defined first coordination sphere, characterized by a precise CN.

The kinetic parameters for the exchange of water and DMF are compared in Table IV. In DMF,[11] the exchange rate does not vary regularly along the series, as is the case in water. This could be explained by an increase in steric crowding of the ligands with the decrease in ionic radii, showed by the mechanistic change from I_d to D along the axis. This variation is also reflected by $\Delta S^{\ddagger}$, going from negative to positive values, and by the change from second- to first-order exchange rate laws. Unfortunately, for water no diluent is sufficiently inert to allow a variable-ligand concentration study in order to obtain the exchange rate laws. However, for the water exchange the rate constants decrease regularly and the $\Delta S^{\ddagger}$ values are negative and fairly constant. Even if a precise activation mode cannot be assigned only by interpreting the sign of $\Delta S^{\ddagger}$, these two observations are consistent with an absence of mechanistic change along the series studied.

Acknowledgment. We thank Dr. Deirdre Hugi-Cleary for her linguistic help. This work was financially supported by the Swiss National Science Foundation (Grant No. 2.854-0.85).

Registry No. $Tb(H_2O)_9{}^{3+}$, 56422-15-2; $Dy(H_2O)_9{}^{3+}$, 56422-19-6; $Ho(H_2O)_9{}^{3+}$, 55664-37-4; $Er(H_2O)_9{}^{3+}$, 56422-25-4; $Tm(H_2O)_9{}^{3+}$, 56422-23-2; $Yb(H_2O)_9{}^{3+}$, 56422-17-4.

Supplementary Material Available: Sample compositions (Table S1), temperature dependence of relaxation rates (Table S2), and temperature dependence of chemical shifts (Table S3) (19 pages). Ordering information is given on any current masthead page.

---

(41) Fay, D. P.; Litchinsky, D.; Purdie, N. *J. Phys. Chem.* **1969**, *73*, 544.

(42) As shown by eq 8, the kinetic effect is proportional to the square of $\Delta\omega_m$; this parameter is small for light lanthanide ions compared to the heavier ones. Determination of the water exchange rates for the early lanthanides by using the same technique is thus not possible.

(43) In water at 298 K, diffusion processes allow the displacement of the water molecules over a distance of one molecular diameter in 5×10^{-12} s, which corresponds to a diffusion limiting rate of 2×10^{11} s^{-1} (see ref 44).

(44) Hertz, H. G. *Prog. Nucl. Magn. Reson. Spectrosc.* **1967**, *3*, 159.

(45) Shannon, R. D. *Acta Crystallogr., Sect. A: Cryst. Phys., Diffr., Theor. Gen. Crystallogr.* **1976**, *A32*, 751.

Contribution from the Institut für Anorganische und Analytische Chemie, Universität Freiburg, 7800 Freiburg, FRG,
and Anorganisch-Chemisches Institut der Technischen Universität München, 8046 Garching, FRG

Dinuclear (Pt,Pt) and Heteronuclear (Pt,Pd) Complexes of Uracil Nucleobases with Identical and Mixed Amine (NH_3, en, bpy) Ligands on the Two Metals. Effects of the Heterometal and Amine on the Oxidizability

Wolfgang Micklitz,[1a] Jürgen Riede,[1b] Brigitte Huber,[1b] Gerhard Müller,[1b] and Bernhard Lippert*[1a]

Received September 8, 1987

The preparation is reported of a series of dinuclear complexes of composition $[(X_2)PtL_2M(Y_2)]Z{\cdot}nH_2O$ with L = 1-methyluracil anion (1-MeU, $C_5H_5N_2O_2$) or 1-methylthymine anion (1-MeT, $C_6H_7N_2O_2$) bound to Pt via the N^3 position and the second metal M (Pt^{II}, Pd^{II}) coordinated through the two O^4 positions of the L ligands. X_2 and Y_2 are any of the following amines: ammonia, $(NH_3)_2$; ethylenediamine, en; 2,2′-bipyridine, bpy. The complexes were characterized by elemental analysis, by spectroscopic methods (IR, Raman, ^1H NMR, UV), and, in the case of *cis*-$[(NH_3)_2Pt(1\text{-}MeU)_2Pd(en)](NO_3)_2{\cdot}6H_2O$ (**4a**), by X-ray analysis. **4a** crystallizes in the triclinic space group $P\bar{1}$, with $a = 11.698$ (2) Å, $b = 11.796$ (2) Å, $c = 12.965$ (2) Å, $\alpha = 114.94$ (1)°, $\beta = 100.29$ (1)°, $\gamma = 111.69$ (1)°, $V = 1383.5$ Å^3, and $Z = 2$. The two 1-MeU ligands adopt a head–head orientation, with *cis*-$Pt(NH_3)_2$ coordination through N^3 and (en)Pd coordination through O^4. The Pt–Pd separation within the cation is 2.927 (1) Å. Dinuclear cations are stacked in such a way that Pt atoms of adjacent dinuclear units face each other (Pt···Pt = 4.553 (1) Å) and likewise Pd atoms are next to each other (Pd···Pd = 3.255 (1) Å). Oxidation of Pt,Pt and Pt,Pd complexes by means of Ce^{IV} in 0.7 M H_2SO_4 has been studied. $[Pt^{II}]_2$ complexes are oxidized without exception to the corresponding $[Pt^{III}]_2$ compounds, whereas $[Pt^{II}Pd^{II}]$ complexes give a mixture of mononuclear $[Pt^{IV}]$ and $[Pd^{II}]$ complexes. With $[Pt^{II}]_2$ complexes, tetranuclear, mixed-valence Pt(2.25) species were observed as intermediates whenever the Y_2 entity was planar ($(NH_3)_2$, bpy), specifically for the following combinations: $X_2 = Y_2 = (NH_3)_2$, $X_2 = Y_2 =$ bpy, $X_2 = (NH_3)_2$ and $Y_2 =$ bpy, $X_2 =$ en and $Y_2 = (NH_3)_2$. In contrast, for $Y_2 =$ en, no Pt(2.25) species were detected by using visible spectroscopy. Standard redox potentials for the respective oxidation steps were determined by use of a standardized Pt electrode. Introduction of en ligands into the dinuclear $[Pt^{II}]_2$ complexes at either side (X_2 and/or Y_2) raised the redox potential for the $[Pt^{II}]_2/[Pt^{III}]_2$ couple relative to that of the $(NH_3)_2$ analogue slightly, while introduction of bpy ligands led to a significant increase in $E°$.

Introduction

Dinuclear Pt^{II} complexes (Chart I, M = Pt) with two bridging cyclic amidate ligands such as deprotonated 1-methylthymine (1-MeT),[2] 1-methyluracil (1-MeU),[3] α-pyridone,[4] α-pyrrolidone,[5] or 1-methylhydantoin[6] in head–head orientations represent suitable

---

(1) (a) Universität Freiburg. (b) Technische Universität München.

(2) (a) Lippert, B.; Neugebauer, D.; Schubert, U. *Inorg. Chim. Acta* **1980**, *46*, L11. (b) Schöllhorn, H.; Thewalt, U.; Lippert, B. *Ibid.* **1984**, *93*, 19.

0020-1669/88/1327-1979$01.50/0

Chart I

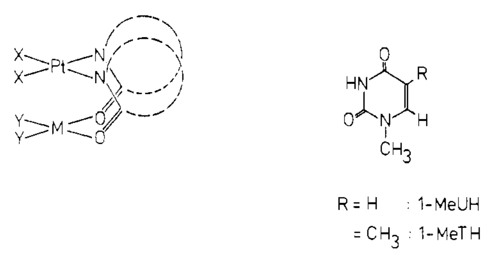

starting materials for the preparation of diplatinum(III),[7-10] mixed-valence-state Pt(2.25)[11,12] and Pt(2.5)[13] compounds, or nonstoichiometric mixtures of these.[14,15]

Previously described Pt,M complexes usually involved two identical metals (M = Pt) *and* two identical amine ligands ($X_2 = Y_2$ = *cis*-$(NH_3)_2$ or ethylenediamine, en) or the two metals. Exceptions were two heteronuclear complexes with M = Cu^{II}, Y = H_2O[16] and M = Zn^{II}, Y = H_2O.[17] In continuation of this work, we have now prepared mixed Pt,Pd complexes containing different amine ligands ($X_2 \neq Y_2$) at the two metals and at the same time a series of Pt_2 complexes of 1-MeU and 1-MeT containing again different amines such as NH_3, ethylenediamine (en), and 2,2′-bipyridine (bpy). These complexes were synthesized in order to study the effects of the heterometal Pd *and* the variation in amine ligands on the oxidizability of the dinuclear unit and also to find out if novel "platinum pyrimidine blues" could be obtained.

Experimental Section

Preparations. $Pt(X_2)Cl_2$ (X_2 = *cis*-$(NH_3)_2$,[18] en,[19] bpy[20]) and $Pd(Y_2)Cl_2$ (Y_2 = en, bpy[21]) were prepared as described. $[Pt(X_2)(H_2O)_2]Z_2$ and $[Pd(Y_2)(H_2O)_2]Z_2$ were prepared in aqueous solution by reaction of the dichloro complexes with 2 equiv of AgZ and filtration of AgCl. *cis*-$(NH_3)_2Pt(1\text{-}MeU)_2{\cdot}4H_2O$ (**1a**)[16] and *cis*-$(NH_3)_2Pt(1\text{-}MeT)_2{\cdot}2.5H_2O$ (**2a**)[22] were prepared as reported. In analogy to **1a** and **2a**, $(en)Pt(1\text{-}MeU)_2{\cdot}5H_2O$ (**1b**) was synthesized from $[(en)Pt(H_2O)_2](NO_3)_2$, to which 2 equiv of NaOH and excess 1-MeUH (3 equiv) had been added. Column chromatography (Sephadex G-10-120) of the crude material gave **1b** in 60% yield (based on Pt). Anal. Calcd for $PtC_{12}H_{28}N_4O_9$: C, 24.21; H, 4.74; N, 14.12. Found: C, 24.20; H, 4.75; N, 14.35. Yellow $(bpy)Pt(1\text{-}MeU)_2{\cdot}4.5H_2O$ (**1c**) was prepared in the very same way in 71% yield. Anal. Calcd for $PtC_{20}H_{29}N_6O_{8.5}$: C, 35.19; H, 3.99; N, 12.31; O, 19.92. Found: C, 34.98; H, 3.98; N, 12.50; O, 20.00. Yellow $(bpy)Pt(1\text{-}MeT)_2{\cdot}4H_2O$ (**2b**) was prepared in analogy to **1c**. Due to low solubility of **2b** in water, column chromatography proved unnecessary, however. Yield: 60%. Anal. Calcd for $PtC_{22}H_{30}N_6O_8$: C, 37.66; H, 4.31; N, 11.98; O, 18.23. Found: C, 37.68; H, 4.12; N, 11.98; O, 17.93.

Table I. List of Dinuclear Pt_2 and Pt,Pd Complexes

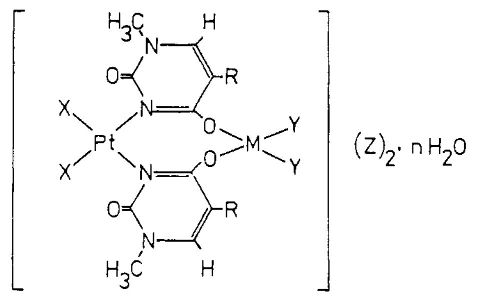

compd	X_2	R	M	Y_2	Z_2	*n*
3	$(NH_3)_2$	H	Pt	en	$(NO_3)_2$	5
4a	$(NH_3)_2$	H	Pd	en	$(NO_3)_2$	2[a]
4b	$(NH_3)_2$	CH_3	Pd	en	$(NO_3)_2$	2
5	$(NH_3)_2$	H	Pt	bpy	$(NO_3)_2$	3
6	$(NH_3)_2$	H	Pd	bpy	$(NO_3)_2$	3
7	en	H	Pt	$(NH_3)_2$	$(ClO_4)_2$	1.5
8	en	H	Pt	en	$(NO_3)_2$	6
9	en	H	Pd	en	SO_4	3
10	en	H	Pd	bpy	$(NO_3)_2$	3
11a	bpy	H	Pt	bpy	$(NO_3)_2$	3
11b	bpy	CH_3	Pt	bpy	$(ClO_4)_2$	4
12	bpy	H	Pd	bpy	$(NO_3)_2$	3.5
13	$(NH_3)_2$	H	Pt	$(NH_3)_2$	$(NO_3)_2$	1

[a] Cf. ref 23 concerning water content.

The dinuclear complexes prepared are listed in Table I and elemental analyses given in Table II. Synthesis of these compounds followed the general route[2,3] of reacting *cis*-X_2PtL_2 with *cis*-$[Y_2M(H_2O)_2]Z_2$. No attempts were made to optimize yields.

$[(NH_3)_2Pt(1\text{-}MeU)_2Pt(en)](NO_3)_2{\cdot}5H_2O$ (3). Reaction conditions: pH 3–4, 48 h, 22 °C, evaporation to dryness and recrystallization from MeOH. Yield: 46%, yellow cubes.

$[(NH_3)_2Pt(1\text{-}MeU)_2Pd(en)](NO_3)_2{\cdot}2H_2O$ (4a). Reaction conditions: pH 2.4, 24 h, 22 °C, concentration to small volume and crystallization by slow evaporation at 3 °C. Yield: 43%, orange-brown crystals. Elemental analysis was performed after 2 days in air.[23]

$[(NH_3)_2Pt(1\text{-}MeT)_2Pd(en)](NO_3)_2{\cdot}2H_2O$ (4b). Reaction conditions: 48 h, 22 °C, concentration to small volume, filtration of precipitate, recrystallization from hot water. Yield: 28%, orange microcrystals.

$[(NH_3)_2Pt(1\text{-}MeU)_2Pt(bpy)](NO_3)_2{\cdot}3H_2O$ (5). Reaction conditions: 24 h, 50 °C, pH 1.8 cooling to 22 °C and filtration of precipitate, recrystallization from water/acetone (2:1). Yield: 47%, red needles.

$[(NH_3)_2Pt(1\text{-}MeU)_2Pd(bpy)](NO_3)_2{\cdot}3H_2O$ (6). Reaction conditions: 24 h, 22 °C, pH 2.2, concentration to a small volume, crystallization at 3 °C. Yield: 61%, orange-red needles.

$[(en)Pt(1\text{-}MeU)_2Pt(NH_3)_2](ClO_4)_2{\cdot}1.5H_2O$ (7). The reaction was carried out under N_2 in N_2-saturated water. Reaction conditions: 2 h, 22 °C, pH 2.3, addition of 1 g of $NaClO_4$ and filtration of the greenish yellow precipitate, recrystallization from water/acetone (2:1). Yield: 13%, yellow cubes.

$[(en)Pt(1\text{-}MeU)_2Pt(en)](NO_3)_2{\cdot}6H_2O$ (8). Reaction conditions: 4 days, 40 °C, pH 2.1, concentration to a small volume, slow evaporation at 3 °C. Yield: 25%, yellow nuggets.

$[(en)Pt(1\text{-}MeU)_2Pd(en)]SO_4{\cdot}3H_2O$ (9). Reaction conditions: 24 h, 22 °C, pH 2.3, evaporation to dryness, redissolving in MeOH at 40 °C,

---

(3) Lippert, B.; Neugebauer, D.; Raudaschl, G. *Inorg. Chim. Acta* **1983**, *78*, 161.

(4) (a) Hollis, L. S.; Lippard, S. J. *J. Am. Chem. Soc.* **1981**, *103*, 1230. (b) Hollis, L. S.; Lippard, S. J. *Ibid.* **1983**, *105*, 3494. (c) Hollis, L. S.; Lippard, S. J. *Inorg. Chem.* **1983**, *22*, 2600.

(5) Matsumoto, K.; Fuwa, K. *J. Am. Chem. Soc.* **1982**, *104*, 897.

(6) Laurent, J.-P.; Lepage, P.; Dahan, F. *J. Am. Chem. Soc.* **1987**, *26*, 1261.

(7) (a) Hollis, L. S.; Lippard, S. J. *J. Am. Chem. Soc.* **1981**, *103*, 6761. (b) Hollis, L. S.; Lippard, S. J. *Inorg. Chem.* **1983**, *22*, 2605. (c) O'Halloran, T. V.; Roberts, M. M.; Lippard, S. J. *Inorg. Chem.* **1986**, *25*, 967.

(8) (a) Lippert, B.; Schöllhorn, H.; Thewalt, U. *J. Am. Chem. Soc.* **1986**, *108*, 525. (b) Schöllhorn, H.; Thewalt, U.; Lippert, B. *J. Chem. Soc., Chem. Commun.* **1986**, 258. (c) Lippert, B.; Schöllhorn, H.; Thewalt, U. *Inorg. Chem.* **1986**, *25*, 407.

(9) Bancroft, D. P.; Cotton, F. A.; Falvello, L. R.; Schwotzer, W. *Inorg. Chem.* **1986**, *25*, 763.

(10) Occasionally, diplatinum(III) complexes have been prepared without prior isolation of diplatinum(II) precursors. See, e.g.: Goodgame, D. M. L.; Rollins, R. W.; Slawin, A. M. Z.; Williams, D. J.; Zard, P. W. *Inorg. Chim. Acta* **1986**, *120*, 91.

(11) (a) Barton, J. K.; Szalda, D. J.; Rabinowitz, H. N.; Waszczak, J. V.; Lippard, S. J. *J. Am. Chem. Soc.* **1979**, *101*, 1434. (b) O'Halloran, T. V.; Mascharak, P. K.; Williams, I. D.; Roberts, M. M.; Lippard, S. J. *Inorg. Chem.* **1987**, *26*, 1261.

(12) (a) Lippert, B.; Neugebauer, D. *Inorg. Chem.* **1982**, *21*, 451. (b) Mascharak, P. K.; Williams, I. D.; Lippard, S. J. *J. Am. Chem. Soc.* **1984**, *106*, 6428. See also ref 11b. (c) Lippert, B.; Schöllhorn, H.; Thewalt, U. *Inorg. Chem.* **1987**, *26*, 1736.

(13) Matsumoto, K.; Takahashi, H.; Fuwa, K. *Inorg. Chem.* **1983**, *22*, 4086. See also ref 5.

(14) Matsumoto, K.; Takahashi, H.; Fuwa, K. *J. Am. Chem. Soc.* **1984**, *106*, 2049.

(15) (a) Matsumoto, K.; Fuwa, K. *Chem. Lett.* **1984**, 569. (b) Matsumoto, K. *Bull. Chem. Soc. Jpn.* **1985**, *58*, 651.

(16) Neugebauer, D.; Lippert, B. *J. Am. Chem. Soc.* **1982**, *104*, 6596.

(17) Schöllhorn, H.; Thewalt, U.; Lippert, B. *Inorg. Chim. Acta* **1985**, *108*, 77.

(18) Dhara, S. G. *Indian J. Chem.* **1970**, *8*, 193.

(19) Basolo, F.; Bailar, J. C., Jr.; Tarr, B. R. *J. Am. Chem. Soc.* **1950**, *72*, 2433.

(20) Morgan, G. T.; Burstall, F. H. *J. Chem. Soc.* **1934**, 965.

(21) McCormick, B. J.; Jaynes, E. N., Jr.; Kaplan, R. I. *Inorg. Synth.* **1972**, *13*, 216.

(22) Lippert, B.; Neugebauer, D. *Inorg. Chim. Acta* **1980**, *46*, 171.

(23) According to the results of the X-ray analysis, **4a** contains (at least) six H_2O groups. This higher water content is consistent with our observation of rapid loss of water in air. Eventually, the anhydrous compound is formed (elemental analysis data).

Table II. Results of Elemental Analyses

compd	% found						% calcd					
	C	H	N	O	Cl/S[b]	Pt,M[c]	C	H	N	O	Cl/S[b]	Pt,M[c]
3	15.33	3.62	15.01	25.76		41.5	15.19	3.61	14.77	25.30		41.2
4a	17.88	3.45	17.32	23.76		37.4	18.08	3.50	17.38	23.82		37.4
4b	20.14	3.75	16.78			36.8	20.16	3.86	16.79			36.2
5	23.47	2.91	13.66	20.34		38.6	23.81	2.99	13.88	20.62		38.7
6	25.93	3.33	15.54	22.84		32.9	26.11	3.29	15.23	22.61		32.8
7	15.02	2.85	11.99	22.25	7.59		15.01	2.83	11.67	22.49	7.38	
8	16.80	3.90	14.11	25.75		39.9	16.94	3.86	14.11	25.79		39.3
9	20.21	3.36[a]	13.46		4.01		20.46	3.95	13.63		3.90	
10	28.05	3.39	14.71	21.93			27.93	3.41	14.81	21.99		
11a	32.04	2.92	12.22	18.16		33.4	32.14	2.88	12.49	18.56		33.9
11b	29.13	2.16[a]	9.09				29.23	2.86	9.16			
12	34.37	3.18	13.28	20.75		29.2	34.28	3.16	13.33	20.55		28.7

[a] H values agree with anhydrous compound only due to use of the Perkin-Elmer 240 elemental analyzer with samples Ar-purged (dehydrated) after weighing. [b] Cl content of **7**; S content of **9**. [c] Sum of metals, determined from combustion residue.

filtration, crystallization at 3 °C (stoppered flask). Yield after 1 day: 19%, yellow microcrystals.

[(en)Pt(1-MeU)$_2$Pd(bpy)](NO$_3$)$_2$·3H$_2$O (10). Reaction conditions: 3 days, 22 °C, pH 2.2, concentration to a small volume, slow evaporation at 3 °C to yield glassy residue and unreacted Pd(bpy) species, recrystallization from warm MeOH. Yield: 15%, brownish red crystals.

[(bpy)Pt(1-MeU)$_2$Pt(bpy)](NO$_3$)$_2$·3H$_2$O (11a). Reaction conditions: 24 h, 50 °C, pH 2.5, evaporatioan to a small volume, filtration of unreacted Pt(bpy) species, addition of 1 g of NaNO$_3$, filtration of precipitate and recrystallization from water. Yield: 36%, red microcrystals.

[(bpy)Pt(1-MeT)$_2$Pt(bpy)](ClO$_4$)$_2$·4H$_2$O (11b). Reaction conditions: 3 days, 80 °C, cooling to 0 °C, filtration of precipitate, recrystallization from water/acetone (5:1). Yield: 39%, red needles.

[(bpy)Pt(1-MeU)$_2$Pd(bpy)](NO$_3$)$_2$·3.5H$_2$O (12). Reaction conditions: 48 h, 22 °C, evaporation to a small volume, crystallization at 3 °C. Yield: 17%, brownish yellow needles.

[(NH$_3$)$_2$Pt(1-MeU)$_2$Pt(NH$_3$)$_2$](NO$_3$)$_2$·H$_2$O (13), was prepared as previously reported.[3] 1-MeUH and 1-MeTH were prepared according to published procedures;[24] 1-MeUH was also obtained in a slightly modified fashion thereof.[25]

Spectroscopy and Solution Studies. IR spectra were recorded on Perkin-Elmer 577 and 783 spectrometers and Raman spectra on a Jobin Yvon U 1000 spectrometer using krypton laser excitation (647.1 nm), and ^{1}H NMR spectra were taken on the following instruments: JEOL JNM-FX 60, Varian T 60 with Nicolet pulse unit, and Bruker SY 200. NMR samples were measured as D$_2$O solutions ([NMe$_4$]$^+$ as internal standard, referenced to sodium 3-(trimethylsilyl)propanesulfonate) or Me$_2$SO-d_6 solutions (TMS as internal standard). UV-vis spectra were recorded on a Perkin-Elmer 555 spectrometer. pH values were measured by use of a glass electrode (Metrohm); for D$_2$O solutions, 0.4 unit was added to the meter reading. The oxidation studies were carried out in 0.7 M H$_2$SO$_4$ in a thermostated vessel at 25 °C with Ce(SO$_4$)$_2$ (dissolved in 0.7 M H$_2$SO$_4$) being the oxidizing agent. Typically, the concentration of the complex to be oxidized was 2 × 10^{-3} M and that of Ce^{IV} was 5 × 10^{-2} M. The Pt combination electrode (Metrohm, Ag/AgCl reference) used to monitor the redox reactions was standardized in a saturated solution of chinhydrone in pH 4 buffer (E = 259 ± 5 mV). For spectrophotometrically monitored oxidations, samples were removed from the reaction vessel, measured in 2-mm cells, and returned to the reaction mixture afterward. To ensure completeness of the reaction, readings of the respective voltages were taken when a constant value was reached (cf. Results, however). No differences in behavior were observed when samples were titrated under N$_2$ instead of air.

Table III. Crystal Data for **4a**

formula	C$_{12}$H$_{24}$N$_{10}$O$_{10}$PdPt·6H$_2$O
fw	877.61
cryst system	triclinic
space group	$P\bar{1}$
a, Å	11.698 (2)
b, Å	11.796 (2)
c, Å	12.965 (2)
α, deg	114.94 (1)
β, deg	100.29 (1)
γ, deg	111.69 (1)
V, Å^3	1383.5
Z	2
d_{calcd}, g cm^{-3}	2.106[a]
μ(Mo Kα), cm^{-1}	58.3
F(000), e	860
temp, °C	−40
radiation	Mo Kα
λ, Å	0.71069
monochromator	graphite
scan	ω
scan width, deg	0.9
scan speed, deg min^{-1}	0.9–29.3
$((\sin\theta)/\lambda)_{max}$, Å^{-1}	0.595
h,k,l range	+13,±14,±15
abs cor	empirical
rel transmission	0.78–1.00
no. of reflcns measd	4872
no. of unique reflcns	4862
R_{int}	0.01
no. of reflcns obsd with $I \geq 2.0\sigma(I)$	4581
no. of params refined	360
R[b]	0.030
R_w[c]	0.044
shift/error max	0.004
$\Delta\rho_{fin}$(max/min), e Å^{-3}	+1.32/−1.12

[a] Density not determined experimentally due to rapid loss of water; cf. also ref 23. [b] $R = \sum(||F_o| - |F_c||)/\sum|F_o|$. [c] $R_w = [\sum w(|F_o| - |F_c|)^2/\sum wF_o^2]^{1/2}$ with $w = 1/\sigma^2(F_o)$.

X-ray Crystallography. A crystal of **4a** (0.3 × 0.25 × 0.15 mm) was sealed under argon at dry ice temperature into a glass capillary. Diffractometer measurements (Syntex P2$_1$) indicated triclinic symmetry, as was confirmed by axial photographs and reduced cell calculations (TRACER). Exact cell constants were obtained by a least-squares fit of the parameters of the orientation matrix to the setting angles of 15 centered high-order reflections. Crystal data and other numbers pertinent to data collection and structure refinement are given in Table III. Data collection, data reduction, and refinement procedures closely followed those described previously.[26] The intensity data were corrected for Lp and absorption effects. For the latter, scans at intervals of 10° around the diffraction vectors of eight selected reflections near χ = 90° were used to evaluate the transmission (Syntex XTL). A correction for decay was not considered necessary, as the repeated measurements of one standard reflection (121) indicated only random intensity fluctuations.

The structure was solved by Patterson methods and completed by Fourier techniques. A total of 12 hydrogen atoms could be located in difference maps, and 12 were calculated at idealized geometrical positions (XANADU). Thereby, found H atoms served to determine the conformations of all NH$_3$ and CH$_3$ groups. Water hydrogens were neglected. Refinement was done with anisotropic displacement parameters with exception of the water molecule O60, which was refined at two half-occupied positions in close proximity with isotropic parameters. The function minimized was $\sum w(|F_o| - |F_c|)^2$. Hydrogen atoms were held constant with U_{iso} = 0.05 Å^2 (SHELX-76).[27] The highest peak in the final

---

(24) Sakai, T. T.; Pogolotti, A. L., Jr.; Santi, D. V. *J. Heterocycl. Chem.* **1968**, *5*, 849.

(25) Micklitz, W.; Lippert, B.; Schöllhorn, H.; Thewalt, U., to be submitted for publication.

(26) Schmidbaur, H.; Schier, A.; Frazão, C. M. F.; Müller, G. *J. Am. Chem. Soc.* **1986**, *108*, 796.

(27) Sheldrick, G. M. "SHELX-76, A Program for Crystal Structure Determination"; University of Cambridge: Cambridge, England, 1976.

Table IV. Fractional Atomic Coordinates and Equivalent Isotropic Displacement Parameters for **4a**[a]

atom	x/a	y/b	z/c	U_{eq}, Å^2
Pt	0.5323 (1)	0.3291 (1)	0.3615 (1)	0.011
Pd	0.4765 (1)	0.0900 (1)	0.1217 (1)	0.013
O21	0.7257 (5)	0.6446 (5)	0.4859 (4)	0.021
O41	0.5229 (5)	0.2539 (5)	0.0905 (4)	0.018
N11	0.7632 (6)	0.6793 (6)	0.3337 (5)	0.018
N31	0.6244 (6)	0.4458 (6)	0.2917 (5)	0.016
C11	0.8423 (8)	0.8344 (8)	0.4211 (6)	0.025
C21	0.7068 (6)	0.5947 (6)	0.3780 (5)	0.012
C41	0.5993 (6)	0.3897 (6)	0.1697 (6)	0.019
C51	0.6542 (8)	0.4810 (8)	0.1271 (6)	0.021
C61	0.7351 (6)	0.6234 (8)	0.2108 (6)	0.022
O22	0.7230 (5)	0.4401 (5)	0.6167 (4)	0.019
O42	0.6748 (4)	0.1702 (5)	0.2185 (4)	0.017
N12	0.8921 (6)	0.4002 (6)	0.5835 (5)	0.020
N32	0.6969 (5)	0.3123 (6)	0.4158 (5)	0.014
C12	0.9699 (8)	0.4862 (9)	0.7193 (6)	0.026
C22	0.7693 (6)	0.3885 (6)	0.5443 (6)	0.016
C42	0.7435 (6)	0.2458 (6)	0.3359 (6)	0.017
C52	0.8714 (6)	0.2607 (8)	0.3814 (6)	0.022
C62	0.9406 (8)	0.3375 (8)	0.5034 (6)	0.025
N10	0.4391 (6)	0.2180 (6)	0.4345 (5)	0.019
N20	0.3729 (5)	0.3563 (6)	0.3153 (5)	0.016
N30	0.4185 (6)	−0.0886 (6)	0.1296 (5)	0.017
N40	0.2804 (6)	−0.0082 (6)	0.0117 (5)	0.020
C10	0.2726 (9)	−0.1539 (10)	0.1020 (9)	0.035
C20	0.2061 (8)	−0.1518 (8)	−0.0051 (8)	0.028
N50	0.6077 (6)	0.4116 (8)	0.8030 (6)	0.027
O51	0.5019 (6)	0.3314 (6)	0.7038 (5)	0.028
O52	0.6718 (6)	0.3585 (6)	0.8327 (6)	0.036
O53	0.6448 (6)	0.5399 (6)	0.8651 (6)	0.041
N60	1.0482 (6)	0.0714 (6)	0.2287 (6)	0.027
O61	0.9765 (6)	0.0040 (6)	0.2665 (5)	0.033
O62	1.1526 (6)	0.0665 (6)	0.2261 (6)	0.032
O63	1.0163 (6)	0.1424 (6)	0.1932 (5)	0.033
O10	0.1460 (6)	0.1712 (6)	0.0337 (6)	0.041
O20	0.9517 (6)	0.2035 (6)	0.7362 (6)	0.041
O30	0.0556 (6)	0.4136 (9)	0.9835 (6)	0.057
O40	0.3012 (6)	0.1257 (8)	0.8480 (6)	0.052
O50	0.6915 (10)	0.1148 (9)	0.6139 (10)	0.066
O601	0.6084 (13)	−0.0582 (13)	0.3317 (12)	0.049
O602	0.5267 (20)	−0.0410 (21)	0.3804 (18)	0.093

[a] $U_{eq} = (U_1 U_2 U_3)^{1/2}$ with U_i being the eigenvalues of the $\mathbf{U}_{ij}$ matrix.

difference map was *not* near the heavy-atom positions and therefore might be an additional partially occupied water molecule. Refinement attempts failed, however. Table IV contains the atomic coordinates.

Neutral, isolated atom scattering factors for all non-hydrogen atoms were those of Cromer and Waber.[28] Scattering factors of the H atoms, based on a bonded spherical atom model, were those of Stewart et al.[29] Corrections for anomalous scattering were applied to all atoms.[30] Reference 26 contains further references to the programs used. All calculations were done on the departmental VAX-780.

Results

Formation. The preparation of *cis*-$[X_2PtL_2MY_2]^{2+}$ (head–head) complexes followed the route previously described by us,[2,3] namely reaction of the neutral complex *cis*-X_2PtL_2, which contains N^3-bound 1-MeU or 1-MeT, with the cationic species *cis*-$[(H_2O)_2MY_2]^{2+}$. Attempts to prepare the isomeric $[X_2ML_2PtY_2]^{2+}$ (M = Pd) complexes failed due to the sensitivity of *cis*-X_2PdL_2 toward H^+, which, at pH 5, led to rapid complex decomposition with formation of free LH ligand. Although, in principle, *cis*-X_2PtL_2 undergoes the same decomposition reaction,[31] it is significant only in strongly acidic medium and even then sufficiently slow to permit isolation of *cis*-$[X_2PtL(LH)]^+$ and a successful competition between the proton and the metal M, respectively. With the exception of *cis*-$[(NH_3)_2Pt(1\text{-MeU})_2Pd(en)](NO_3)_2$ (**4a**), for which the composition was also confirmed by X-ray analysis, all other compounds were characterized by use of elemental analysis and IR Raman, and ^1H NMR spectroscopy.

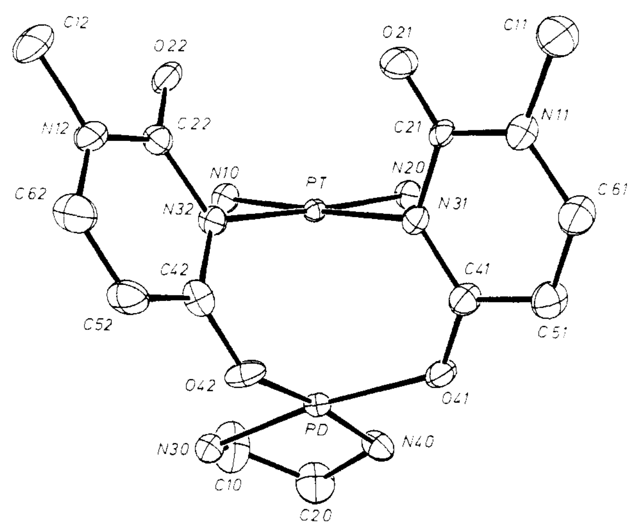

Figure 1. Molecular structure of the cation *cis*-$[(NH_3)_2Pt(1\text{-MeU})_2Pd(en)]^{2+}$ (head–head) of **4a** (ORTEP; displacement parameters at the 50% probability level; H atoms omitted for clarity).

Table V. Selected Interatomic Distances (Å) and Angles (deg) for **4a**

Pt···Pd	2.927 (1)		
Pt–N31	2.044 (5)	Pt–N32	2.040 (5)
Pt–N20	2.035 (5)	Pt–N10	2.040 (6)
Pd–O41	2.039 (4)	Pd–O42	2.046 (4)
Pd–N40	2.028 (6)	Pd–N30	2.015 (5)
N11–C11	1.453 (9)	N12–C12	1.481 (9)
N11–C21	1.376 (8)	N12–C22	1.369 (9)
C21–O21	1.205 (8)	C22–O22	1.220 (8)
C21–N31	1.404 (8)	C22–N32	1.404 (8)
N31–C41	1.354 (8)	N32–C42	1.348 (9)
C41–O41	1.283 (8)	C42–O42	1.283 (8)
C41–C51	1.413 (9)	C42–C52	1.42 (1)
C51–C61	1.35 (1)	C52–C62	1.33 (1)
C61–N11	1.360 (9)	C62–N12	1.35 (1)
N40–C20	1.485 (9)	N30–C10	1.49 (1)
C10–C20	1.48 (1)		
N31–Pt–N32	90.6 (2)	N10–Pt–N20	89.9 (2)
N31–Pt–N20	88.9 (2)	N32–Pt–N10	90.5 (2)
O41–Pd–O42	91.2 (2)	N30–Pd–N40	84.0 (2)
O41–Pd–N40	91.4 (2)	O42–Pd–N30	92.9 (2)
Pt–N31–C41	123.8 (4)	Pt–N32–C42	123.3 (4)
Pt–N31–C21	115.0 (4)	Pt–N32–C22	115.7 (4)
C21–N31–C41	120.8 (5)	C22–N32–C42	120.7 (5)
N31–C41–O41	120.9 (6)	N32–C42–O42	121.0 (6)
C41–O41–Pd	127.9 (4)	C42–O42–Pd	129.9 (4)

IR and Raman Spectra. IR and Raman spectra (solid state) of Pt_2 and Pt,Pd complexes did not show major differences as far as the nucleobase vibrations were concerned but expectedly displayed differences in the region below 500 cm^{-1}. The Raman modes around 810 and 625 cm^{-1}, previously found to be indicative of N^3,O^4-bridging of 1-MeU,[3] were observed in all Pt_2 and Pt,Pd complexes and did not differ greatly between analogous compounds, e.g. 814 and 625 cm^{-1} in **8** and 806 and 622 cm^{-1} in **9**. For a representative example, see the supplementary material. In the double bond stretching region of the IR, the spectroscopic changes described for the 1-MeT system[22] also apply to 1-MeU complexes and do not differ greatly between Pt_2 and Pt,Pd complexes. In particular, the broad and intense band of neutral 1-MeUH at 1660 cm^{-1}, which is split into two well-separated components on N^3 platinum binding (centered at 1650 and 1560 cm^{-1}), undergoes a characteristic further separation on covalent metal binding at O^4 (1650 and ca. 1520 cm^{-1}; cf. supplementary material).

---

(28) Cromer, D. T.; Waber, J. T. *Acta Crystallogr.* **1965**, *18*, 104.

(29) Stewart, R. F.; Davidson, E. R.; Simpson, W. T. *J. Chem. Phys.* **1965**, *42*, 3175.

(30) *International Tables for X-ray Crystallography*; Kynoch: Birmingham, England, 1974; Vol. 4.

(31) (a) Lippert, B. *Inorg. Chim. Acta* **1981**, *55*, 5. (b) Schöllhorn, H.; Thewalt, U.; Lippert, B., unpublished results.

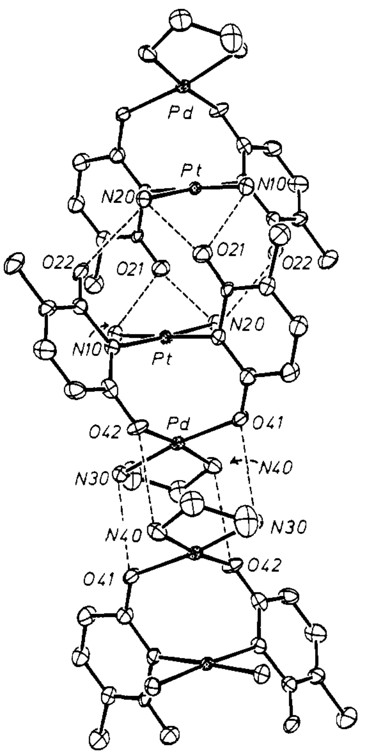

Figure 2. Strandlike arrangement of cations of **4a** in the crystal. Broken lines indicate hydrogen-bonding interactions.

Crystal and Molecular Structure of *cis*-[$(NH_3)_2Pt$(1-MeU)$_2$Pd(en)]$(NO_3)_2\cdot 6H_2O$ (4a). A view of the molecular cation of **4a** is given in Figure 1, and selected interatomic distances and angles are listed in Table V. The dinuclear cation consists of a *cis*-$(NH_3)_2Pt^{II}$ moiety bound to the N^3 positions of two 1-methyluracilato ligands and an (en)Pd^{II} moiety coordinated to two O^4 sites of the same ligands, forcing the heterocyclic rings into head–head orientation. Within the dinuclear cation, the two metals are 2.927 (1) Å apart. There is no apparent disorder with respect to the mutual interchange of the two different metals, consistent with the way of preparation and the inertness of Pt^{II}. The coordination geometry of both metals is square planar, with the metal atoms being displaced slightly from their respective best coordination planes *toward* each other (Pt, 0.04 Å; Pd, 0.10 Å). The coordination planes are tilted by 34.2° and substantially twisted about the Pt–Pd vector (torsion angles N3–Pt–Pd–O4 of −18.3 and −16.3°) and in this respect are similar to those of other diplatinum(II) complexes.[2b] The 1-MeU rings are essentially planar. The metal atoms are considerably out of the ligand planes, however (Pt, 0.20 and 0.35 Å; Pd, 0.62 and 0.46 Å). The 1-MeU rings are roughly at right angles to each other (dihedral angle 96.4°). Pt–N and Pd–N distances are normal and not significantly different from the Pd–O bonds.

As to the packing of the dinuclear PtPd cations in **4a**, infinite strands of the head–head dimers are observed in a sequence · (Pt,Pd)·(Pd,Pt)·(Pt,Pd)· (Figure 2). Thereby, the respective metal centers are centrosymmetrically related. The intermolecular distances are 4.553 (1) Å for the Pt atoms and, surprisingly short, 3.255 (1) Å for the Pd atoms. Thus, **4a** displays a packing pattern observed in both type I[2b] and type II diplatinum(II) complexes, with distances of N_2MO_2 planes facing each other considerably shorter than those of N_4M planes.

There is extensive hydrogen bonding between the cations themselves (indicated as broken lines in Figure 2) and also between cations, nitrate anions, and water molecules. Table VI summarizes some of their geometrical parameters.[32] Due to the center of symmetry between the related Pt and Pd centers, there exist no less than four hydrogen bonds between pairs of dinuclear cations. One, which involves H21, probably is bifurcated.

Table VI. Hydrogen-Bonding Interactions for **4a**[a]

H bond	dist H···O, Å	angle at H, deg	acceptor
N10–H11···O51	2.36	129	NO_3^-
N10–H12···O50[1]	2.57	142	H_2O
N10–H13···O21[2]	2.11	155	1-MeU
N20–H21···O21[2]	2.21	136	1-MeU
N20–H21···O22[2]	2.27	119	1-MeU
N20–H22···O62[3]	2.30	126	NO_3^-
N20–H22···O10	2.46	142	H_2O
N20–H23···O53[2]	2.29	139	NO_3^-
N30–H31···O41[4]	2.18	147	1-MeU
N30–H32···O601	2.17	137	H_2O (disord)
N30–H32···O602	2.19	146	H_2O (disord)
N40–H41···O42[4]	2.38	127	1-MeU
N40–N41···O40[5]	2.35	138	H_2O
N40–H42···O10	2.18	147	H_2O

[a] Symmetry transformations: (1) $1-x, -y, 1-z$; (2) $1-x, 1-y, 1-z$; (3) $x-1, y, z$; (4) $1-x, -y, -z$; (5) $x, y, z-1$.

^1H NMR Spectra. With 1-MeU complexes, N^3 coordination of the X_2Pt moieties in all cases was deduced from ^4J coupling between ^{195}Pt and H5 (≃14 Hz). Whenever ethylenediamine was bound to Pt (in X_2Pt or PtY_2), ^3J coupling between ^{195}Pt and $-CH_2-$ of the en ligand was observed. Coupling constants were different, however, for these two arrangements: With Y_2 = en, the situation with en trans to two O4 oxygens, ^3J values were larger by about 10 Hz as compared to X_2 = en, with en trans to two N3 nitrogens (52 vs 42 Hz). These values compare well with those reported for $[enPt(H_2O)]^{2+}$ and $enPtL_2$ systems (L = nitrogen donor)[33] and probably reflect the differences in trans influence of N and O donor atoms rather than differences in conformations of the en chelate rings in the two positions. As with *cis*-[$(NH_3)_2Pt$(1-MeU)$_2Pt(NH_3)_2]^{2+}$ (**13**),[3] H5 and H6 resonances of the bridging 1-MeU ligands are shifted downfield relative to those of *cis*-X_2Pt(1-MeU)$_2$, H5 slightly more so than H6. Substitution of M = Pt^{II} by Pd^{II} gave qualitatively similar spectra, with shifts closer to those of *cis*-X_2Pt(1-MeU)$_2$, however, (cf. supplementary material). Spectra recorded in Me_2SO-d_6 (compounds **5** and **6**) confirmed this observation. Mixtures of *cis*-$(NH_3)_2Pt$(1-MeU)$_2$ (**1a**) and the Pt,Pd complex **4a** gave two sets of resonances due to the two components, indicating that **4a** is nonlabile on the NMR time scale. Since in the ^1H NMR spectrum of **4a**, as in the case of the other Pt,Pd complexes, resonances due to *cis*-$(NH_3)_2Pt$(1-MeU)$_2$ were not detected, the equilibrium

$$\mathbf{4a} \overset{D_2O}{\rightleftharpoons} \mathbf{1a} + [(en)Pd(D_2O)]^{2+}$$

must be far to the left under the conditions of the NMR experiment (≃0.1 M, 30 °C). On the other hand, the reduction in downfield shift of H5 in Pt,Pd complexes as compared to the corresponding Pt_2 complexes (**3** vs **4a**, **8** vs **9**) suggest a weaker interaction of Pd^{II} with the O^4 sites of 1-MeU. In agreement with this picture is also the observation that (en)Pd^{II} in **4a** is instantaneously substituted by Ag^+ with formation of a poorly soluble heteronuclear complex, *cis*-[$(NH_3)_2Pt$(1-MeU)$_2$Ag]NO_3.[22,34]

With Y_2 = bpy, 1-MeU resonances in $[X_2PtL_2PdY_2]^{2+}$ are shifted further downfield as compared to Y_2 = en (**10** vs **9**). With $X_2 = Y_2$ = bpy (**12**), this trend is even more pronounced. The same holds true for the dinuclear Pt_2 complexes, with 1-MeU resonances of [(bpy)Pt(1-MeU)$_2$Pt(bpy)]$^{2+}$ (**11a**) *shifted the most* of all dinuclear complex resonances studied. Resonances of **11a** relative to those of **13** ($X_2 = Y_2 = (NH_3)_2$) occur downfield by 0.18 ppm (CH_3), 0.43 ppm (H5), and 0.34 ppm (H6). These shifts probably are due to ring-current effects of the bpy ligand(s) and/or increased metal–donor atom interactions as a consequence of

---

[32] Since the hydrogen atoms were not refined, the numbers given in Table VI should be considered guidelines. Distances between heavy atoms of each hydrogen bond are around 3 Å.

[33] (a) Appleton, T. G.; Hall, J. R. *Inorg. Chem.* **1971**, *10*, 1717. (b) Lippert, B. *Inorg. Chem.* **1981**, *20*, 4326.

[34] The rather low solubility of the Pt,Ag complex may contribute to the facile substitution of Pd by Ag.

favorable metal–bpy back-bonding.

UV Spectra. N^3 Pt binding does not affect the 1-MeU absorptions in the 200–300-nm range (1-MeUH, 267.5 nm; 1-MeU, 265 nm; *cis*-$(NH_3)_2Pt(1\text{-}MeU)_2$, 264 nm), and neither do variations at the amine side of X_2PtL_2 (X_2 = en, 262 nm; X_2 = bpy, 260 nm). Significant red shifts of this band are observed, however, on binding of an electrophile to the exocyclic oxygens, notably O^4: Addition of Ag^+ or Zn^{2+}, for which coordination at O^4 is documented in the solid state,[17,35] leads to the appearance of new absorptions around 285 nm. Likewise, the UV spectra of the mixed Pt,Pd complexes **4a** and **9** display two absorptions at 264 and 285 nm. Variations in concentrations of X_2PtL_2 and $[(en)Pd(H_2O)_2]^{2+}$ allow an assignment of the 285-nm band as due to the intact dinuclear complexes and, at the same time, indicate that under conditions of the UV experiment ($\simeq 4 \times 10^{-4}$ M), complexes **4a** and **9** are largely dissociated into their components. Similarly, for Pt,Zn[17] and Pt_2Mn[36] complexes, dissociation reactions have been observed. Pt,Pd complexes containing bpy ligands at the Pd metal (**6**, **10**) are more stable than their ethylenediamine analogues, considering the higher intensity of the red-shifted component.

Oxidative Titrations of Mononuclear Pt Complexes. Oxidations of mono- and dinuclear complexes were performed by use of Ce^{IV} in 0.7 M H_2SO_4 and followed potentiometrically or spectrophotometrically or both ways simultaneously. The Pt indicator electrode was standardized before each titration, thus permitting the determination of standard redox potentials $E°$ from the titration curves at half-oxidation. Values obtained this way for the oxidation of K_2PtCl_4 ($E° = 700 \pm 8$ mV vs Ag/AgCl) were well reproducible, and the $E°$ for Ce^{III}/Ce^{IV} obtained experimentally[37] (1225 mV vs Ag/AgCl; 1447 mV vs H/H^+) is in excellent agreement with literature data (1440 mV in 1 N H_2SO_4).[38] With *cis*-$(NH_3)_2PtCl_2$, $E°$ displayed some variation depending on the rate of Ce^{IV} addition: More rapid addition of Ce^{IV} (3–6-min intervals)[39] gave higher values than slow addition (40-min intervals), in which case a value $E° = 645 \pm 15$ mV (vs Ag/AgCl) was found. $E°$ values for the two Pt compounds are somewhat lower than those reported in 0.1 N HCl.[40]

Amounts of consumed Ce^{IV} solutions at the end point of each titration did not indicate that oxidation of Cl^- ligands of K_2PtCl_4 and *cis*-$(NH_3)_2PtCl_2$ had taken place, as has been observed for HCl.[41]

For the oxidation of $(en)Pt(1\text{-}MeU)_2$ and *cis*-$(NH_3)_2Pt(1\text{-}MeU)_2$ (and their respective protonated forms $[X_2Pt(1\text{-}MeU)(1\text{-}MeUH)]^+$)[31b] to the corresponding Pt^{IV} complexes, $E°$ values of 812 and 836 mV (vs Ag/AgCl) were determined. Consistent with findings of Kukushkin and Dkhara,[42] (i) the en complex is oxidized more easily than the $(NH_3)_2$ complex, and (ii) the presence of the heterocyclic 1-MeU ligand shifts $E°$ to higher values when compared with those of Pt^{II} compounds containing exclusively primary or secondary amine ligands.

Oxidation of Pt_2 Complexes. Oxidation of the dinuclear Pt^{II} complexes with Ce^{IV} gave differing results, depending on the nature of the amine ligands and their relative attachment (trans to N^3 or O^4 of 1-MeU).

***cis*-$[(NH_3)_2Pt(1\text{-}MeU)_2Pt(NH_3)_2](NO_3)_2\cdot H_2O$ (13).** This compound, which contains two identical X_2, Y_2 groups and which has been shown to form a Pt(2.25) blue[12] and diplatinum(III) species[8] on chemical oxidation, was studied for comparison with

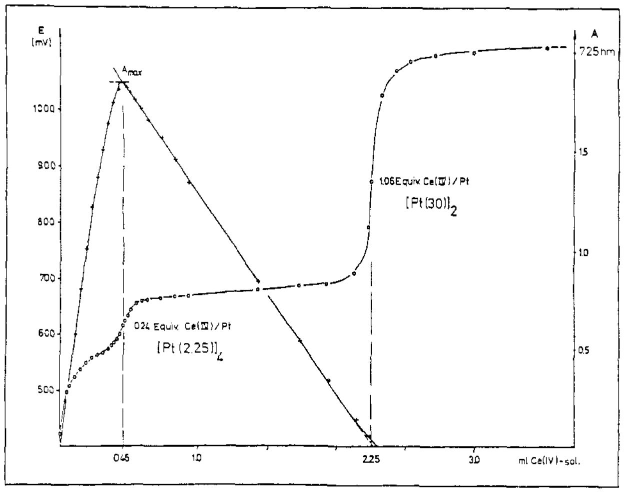

Figure 3. Titration curves of the cation *cis*-$[(NH_3)_2Pt(1\text{-}MeU)_2Pt(NH_3)_2]^{2+}$ of **13** with Ce^{IV} in 0.7 M H_2SO_4, monitored potentiometrically ($E°$ vs mL of Ce^{IV}) and spectrophotometrically (A_{725nm} vs mL of Ce^{IV}).

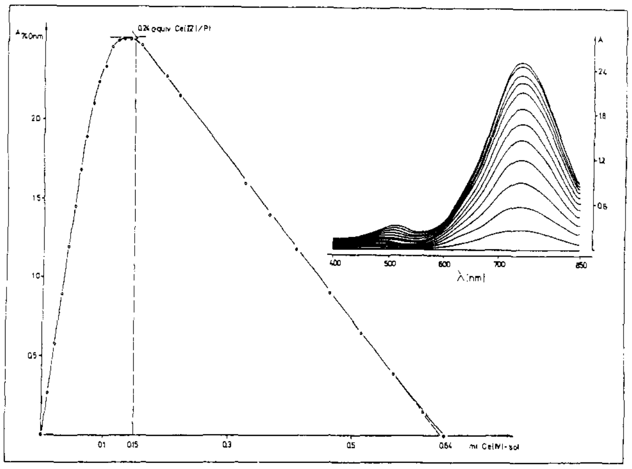

Figure 4. Intensity of 740-nm-absorption of Pt(2.25) species derived from the cation $[(en)Pt(1\text{-}MeU)_2Pt(NH_3)_2]^{2+}$ of **7**, as a function of added Ce^{IV} until a maximum is reached (insert) and as plotted against consumption of Ce^{IV} solution. Visible spectra were recorded at constant intervals of 3 min.

the mixed-amine complexes. Ce^{IV} oxidation of **13** proceeds in two steps with consumption of ca. 0.25 equiv of Ce^{IV}/Pt and an additional 0.75 equiv/Pt, respectively (Figure 3). This behavior is consistent with the reaction sequence

$$\underset{\mathbf{13}}{2[Pt^{II}]_2} \xrightarrow{+1Ce^{IV}} \underset{\mathbf{13a}}{[Pt^{III}(Pt^{II})_3]} \xrightarrow{+3Ce^{IV}} \underset{\mathbf{13b}}{2[Pt^{III}]_2}$$

During the titration with Ce^{IV}, the color of the sample changes from initially yellow via blue-green, green, olive black, and reddish black to orange-red and yellow. Formation of the Pt(2.25) intermediate **13a** was simultaneously followed by visible spectroscopy. The intensity of the main absorption of **13a** at 725 nm (compared to 740 nm in diluted HNO_3)[12c] reached a maximum after addition of 0.255 equiv of Ce^{IV}/Pt and declined linearly with continuous addition of Ce^{IV}. Titration of **13a**, prepared by HNO_3 oxidation of **13**[12b] and redissolved in 0.7 M H_2SO_4, displayed the identical drop in 725-nm intensity on addition of Ce^{IV}. The $E°$ values for the process **13** → **13a** were 560 mV (taken from an E vs mL of Ce^{IV} plot) and 565 mV (potential at which the 725-nm absorption reached half-maximum), and those for the step **13** → **13b** were found to be 685 and 690 mV, respectively (vs Ag/AgCl).[43]

---

[35] Goodgame, D. M. L.; Rollins, R. W.; Lippert, B. *Polyhedron* **1985**, *4*, 829 and references cited therein.

[36] Lippert, B.; Schubert, U. *Inorg. Chim. Acta* **1981**, *56*, 15.

[37] Determined after addition of 4 equiv of Ce^{IV}/Pt^{II}, giving a Ce^{III}/Ce^{IV} ratio of 1.

[38] Seel, F. *Grundlagen der analytischen Chemie*; Verlag Chemie: Weinheim, West Germany, 1979; p 377.

[39] Addition of Ce^{IV} in 10–20-μL steps (5×10^{-2} M)/7–10 mg of Pt species.

[40] Grünberg, A. A.; Lawrentiew, W. N.; Ptizyn, B. W. *Dokl. Akad. Nauk SSSR* **1940**, *26*, 52.

[41] Ramstad, T.; Woollins, J. D.; Weaver, M. J. *Inorg. Chim. Acta* **1986**, *124*, 187.

[42] Kukushkin, Yu. N.; Dkhara, S. Ch. *Russ. J. Inorg. Chem.* (*Engl. Transl.*) **1970**, *15*, 813.

[43] Unlike the first oxidation step, potentials of the second step (**13b** → **13c**) displayed a time dependence (dropping with time) and gave constant values after ca. 30 min only.

$[(en)Pt(1\text{-}MeU)_2Pt(NH_3)_2](ClO_4)_2\cdot1.5H_2O$ (7). Ce^{IV} oxidation of **7** was qualitatively similar to that of **13**, indicative of a two-step process involving a Pt(2.25) intermediate, the visible spectrum of which also resembled that of **13a** closely (Figure 4). Unlike in the case of **13**, however, the titration curve ($E°$ vs mL of Ce^{IV}) did not display a distinct step for the Pt(2.0) → Pt(2.25) process, presumably because $E°$ values of the two oxidation processes are too close to produce well-resolved steps. As a consequence, the $E°$ value for the first oxidation step (695 mV, taken as the potential measured at the time when the 740-nm absorption had reached 50% of its final intensity) almost certainly is too high, and the same applies to the calculated $E°$ for the $[Pt^{II}]_2/[Pt^{III}]_2$ couple (see below). Another problem of accurately determining $E°$ values of the two redox processes came from the gradual decomposition of the Pt(2.25) species: Long intervals ($\geqslant$30 min) between Ce^{IV} portions eventually gave lower potentials, but at the same time the visible spectrum indicated that the Pt(2.25) complex had decayed partially.

***cis*-$[(NH_3)_2Pt(1\text{-}MeU)_2Pt(en)](NO_3)_2\cdot5H_2O$ (3).** The interchange of en and $(NH_3)_2$ ligands in **7**, which gave **3**, resulted in a dramatic loss of complex stability of the Pt(2.25) species: No stable Pt(2.25) species was formed when **3** was treated with Ce^{IV} but a transient only species (purple; λ_{max} 790 nm), which decayed within minutes after its formation. An end point was reached after 2 equiv of Ce^{IV}/diplatinum(II) complex had been added, consistent with the reaction

$$[Pt^{II}]_2 \xrightarrow[-2Ce^{III}]{+2Ce^{IV}} [Pt^{III}]_2$$

The $E°$ value derived from the titration curve was 656 mV.

$[(en)Pt(1\text{-}MeU)_2Pt(en)](NO_3)_2\cdot6H_2O$ (8). No formation of any green, blue, or purple intermediate was observed during the titration of **8** with Ce^{IV}. Rather, the solution stayed yellow. A sharp rise in potential was observed when 1 equiv of Ce^{IV}/Pt had been added, again indicating oxidation of the diplatinum(III) complex ($E°$ = 690 mV). Dissociation of **8** into $(en)Pt(1\text{-}MeU)_2$ and $[(en)Pt(H_2O)_2]^{2+}$ and individual oxidation to the respective Pt^{IV} complexes could be ruled out, since it would have required twice the amount of Ce^{IV} than actually used up.

***cis*-$[(NH_3)_2Pt(1\text{-}MeU)_2Pt(bpy)](NO_3)_2\cdot3H_2O$ (5).** Oxidation of this complex to the diplatinum(III) complex proceeded via a stable Pt(2.25) intermediate (purple, λ_{max} 568 nm (ϵ 11 000 M^{-1} cm^{-1}), 800 (26 000); c 1.9×10^{-4} mol L^{-1}). $E°$ values were 703 and 935 mV for the two steps.

$[(bpy)Pt(1\text{-}MeU)_2Pt(bpy)](NO_3)_2\cdot3H_2O$ (11a). Again, oxidation with Ce^{IV} gave an intensely purple Pt(2.25) intermediate (λ_{max} 578 nm (ϵ 19 200 M^{-1} cm^{-1}), 763 (21 900)) prior to formation of the orange-yellow diplatinum(III) complex. $E°$ values were 735 and 998 mV.

Behavior of Pd-Containing Complexes. No oxidation through Ce^{IV} was detected for any of the following mononuclear Pd^{II} complexes: $K_2[PdCl_4]$, $(bpy)Pd(1\text{-}MeU)_2$, $[(en)Pd(H_2O)_2]^{2+}$, and $[Pd(H_2O)_4]^{2+}$.[44] Likewise, attempts to oxidize the mixed Pt,Pd complexes to $Pt^{III}Pd^{III}$ complexes were unsuccessful. Rather, the heteronuclear complexes dissociated under the "influence" of Ce^{IV} according to

$$[X_2Pt^{II}L_2Pd^{II}Y_2]^{2+} \xrightarrow[-2Ce^{III}]{+2Ce^{IV},\ H_2O} [X_2PtL_2(OH_2)_2]^{2+} + [(OH_2)_2PdY_2]^{2+}$$

and only Pt^{II} was oxidized to Pt^{IV} with consumption of exactly 2 equiv of Ce^{IV}/Pt. $E°$ values taken from the titration curves were virtually identical with those obtained for the mononuclear $(X_2)Pt(1\text{-}MeU)_2$ complexes (see above). With Y_2 = bpy (**6**, **10**), formation of a yellow precipitate containing the Pd(bpy) entity took place. In the case of *cis*-$[(NH_3)_2Pt(1\text{-}MeU)_2Pd(en)](NO_3)_2\cdot2H_2O$ (**4a**), formation of a small amount (5%) of the novel trinuclear, mixed-valence-state compound $[(NH_3)_2Pt(1\text{-}MeU)_2Pd(1\text{-}MeU)_2Pt(NH_3)_2]^{3+}$ was detected spectrophotometrically, consistent with one method of its preparation from a HNO_3-acidified solution of **4a**.[45]

Table VII. $E°$ Potentials (mV vs Ag/AgCl) of Dinuclear Pt Complexes $[(X_2)Pt(1\text{-}MeU)_2Pt(Y_2)]^{2+/n+}$ (Head–Head)

compd	X_2	Y_2	Pt(2.0)/ Pt(2.25)	Pt(2.25)/ Pt(3.0)	Pt(2.0)/ Pt(3.0)
13	$(NH_3)_2$	$(NH_3)_2$	558,[a] 554[b]	682,[a] 680[b]	651,[c] 649[d]
3	$(NH_3)_2$	en			656
8	en	en			690
7	en	$(NH_3)_2$	<695[b,c]	735[b]	<725[d,e]
5	$(NH_3)_2$	bpy	703,[a] 703[b]	933,[a] 935[b]	876,[c] 877[d]
11a	bpy	bpy	735[b]	998[b]	932[d]

[a] Taken from titration curve ($E°$ vs mL of Ce^{IV}). [b] Taken from visible spectra ($A_{50\%}$ vs $E°$). [c] Calculated from values obtained according to footnote *a*. [d] Calculated from values obtained according to footnote *b*. [e] Value questionable; cf. text.

Discussion

Dinuclear complexes of composition $[(X_2)Pt(1\text{-}MeU)_2Pt(Y_2)]^{2+}$, with X_2, Y_2 = identical or different amine ligands and the 1-MeU ligands arranged head–head, are oxidized in 0.7 M H_2SO_4 by Ce^{IV} to the corresponding diplatinum(III) complexes. Oxidation beyond this stage, to Pt^{IV} complexes, was not observed. In several cases, oxidation proceeded via strongly colored mixed-valence intermediates that, in analogy to the structurally characterized 1-MeU–Pt(2.25) blue,[11b] most likely are of the dimer-of-dimer type $[Pt^{III}(Pt^{II})_3]$ as well. No evidence for a stable Pt(2.5) species, as claimed for $X_2 = Y_2 = (NH_3)_2$[41] and reported for α-pyrrolidonato complexes,[13] has been found. It appears that a planar Y_2 moiety ($(NH_3)_2$, bpy) facilitates formation of a Pt(2.25) species (cf. oxidation behavior of **5**, **7**, **11a**, and **13**), presumably because of the good approach of two head–head dimers via their O_2PtN_2 faces. In contrast, the puckering of the ethylenediamine ligands in complexes with Y_2 = en (**3**, **8**) makes such an approach and consequently the interaction between the Pt d_{z^2} orbitals of adjacent dimers more difficult and does not lead to a stable Pt(2.25) species under the conditions applied.[46]

Table VII summarizes the $E°$ values for the individual oxidation steps, Pt(2.0)/Pt(2.25), Pt(2.25)/Pt(3.0), and Pt(2.0)/Pt(3.0). Unless determined experimentally, as with **3** and **8**, potentials of the Pt(2.0)/Pt(3.0) couples were calculated according to

$$E°_{Pt(2.0)/Pt(3.0)} = \frac{E°_{Pt(2.0)/Pt(2.25)} + 3E°_{Pt(2.25)/Pt(3.0)}}{4}$$

$E°$ values for Pt(2.0)/Pt(3.0) are in a relatively narrow range for NH_3- and en-containing complexes, yet considerably higher with bpy-containing compounds. Absolute values for $(NH_3)_2$-containing 1-MeU complexes are close to the value reported for the analogous α-pyridone complex (0.63 V vs SCE).[7a,b] Unlike in mononuclear complexes of Pt^{II}, in diplatinum(II) complexes substitution of $(NH_3)_2$ by en appears to make oxidation to the diplatinum(III) complex more difficult. A feasible explanation would be that the steric demand of the en ligand at either side of the dinuclear complex and particularly on both sides of the dinuclear complex is responsible for this trend. Structural differences of diplatinum(III) complexes containing exclusively NH_3 or en ligands seem to support such a view.[7c]

Attempts to generate mixed Pt^{III},Pd^{III} complexes containing bridging 1-MeU ligands failed. Instead, Pt^{II} was oxidized to Pt^{IV} with Pd^{II} unchanged and the dinuclear complex cleaved. We note that while mixed Pd^{II},Pd^{III} species have been electrogenerated,[47] the synthesis of $[Pd^{III}]_2$ containing four substituted formamidinato ligands has been unsuccessful as well.

Acknowledgment. This work has been supported by the Deutsche Forschungsgemeinschaft, the Fonds der Chemischen

---

(44) Elding, L. I. *Inorg. Chim. Acta* **1972**, *6*, 647.

(45) Micklitz, W.; Müller, G.; Riede, J.; Lippert, B *J. Chem. Soc., Chem. Commun.* **1987**, 76.

(46) Isolation of a Pt(2.25) blue containing en ligands may nevertheless be possible (cf. comproportionation reaction between $[Pt^{II}]_2$ and $[Pt^{III}]_2$ in ref 11b).

(47) Cotton, F. A.; Matusz, M.; Poli, R. *Inorg. Chem.* **1987**, *26*, 1472.

Industrie, and Degussa (loan of K_2PtCl_4). We thank G. Trötscher and H. Hillebrecht for experimental assistance.

Registry No. **1a**, 83350-97-4; **1b**, 113705-71-8; **1c**, 113705-74-1; **2a**, 74539-69-8; **2b**, 113705-76-3; **3**, 113705-50-3; **4a**, 113705-51-4; **4b**, 113705-53-6; **5a**, 113705-55-8; **6**, 113705-57-0; **7**, 113705-59-2; **8**, 113705-61-6; **9**, 113705-62-7; **10**, 113705-64-9; **11a**, 113705-66-1; **11b**, 113705-68-3; **12**, 113705-70-7; **13**, 85886-74-4; **13a**, 92220-61-6; **13b**, 113705-77-4; $[(NH_3)_2Pt(1\text{-}MeU)_2Pt(en)]^{4+}$, 113705-78-5; $[(en)Pt(1\text{-}MeU)_2Pt(en)]^{4+}$, 113725-93-2; $[(en)Pt(1\text{-}MeU)_2Pt(NH_3)_2]^{4+}$, 113705-79-6; $[(NH_3)_2Pt(1\text{-}MeU)_2Pt(bpy)]^{4+}$, 113705-80-9; $[(bpy)Pt(1\text{-}MeU)_2Pt(bpy)]^{4+}$, 113705-85-4; $[(en)Pt(1\text{-}MeU)_2Pt(NH_3)_2]_2{}^{5+}$, 113705-82-1; $[(NH_3)_2Pt(1\text{-}MeU)_2Pt(bpy)]_2{}^{5+}$, 113705-83-2; $[(bpy)Pt(1\text{-}MeU)_2Pt(bpy)]_2{}^{5+}$, 113705-84-3; *cis*-$Pt(NH_3)_2Cl_2$, 15663-27-1; $Pt(en)Cl_2$, 14096-51-6; $Pt(bpy)Cl_2$, 13965-31-6; $Pd(en)Cl_2$, 15020-99-2; $Pd(bpy)Cl_2$, 14871-92-2; $[Pd(bpy)(H_2O)_2](NO_3)_2$, 113705-73-0; $[Pd(en)(H_2O)_2]SO_4$, 113705-75-2; $[Pt(NH_3)_2(H_2O)_2](NO_3)_2$, 52241-26-6; $[Pt(en)_2(H_2O)_2](ClO_4)_2$, 33728-67-5; $[Pt(en)_2(H_2O)_2](NO_3)_2$, 52241-27-7; $[Pt(bpy)_2(H_2O)_2](NO_3)_2$, 64800-95-9; $[Pt(bpy)_2(H_2O)_2](ClO_4)_2$, 54822-53-6; $[Pd(en)(H_2O)_2](NO_3)_2$, 62418-53-5; $[(NH_3)_2Pt(1\text{-}MeU)_2Pd(1\text{-}MeU)_2Pt(NH_3)_2]^{3+}$, 113705-81-0.

Supplementary Material Available: Listings of positional and thermal parameters for **4a** and ^1H NMR shifts of mono- and dinuclear complexes, Raman spectra of **8** and **9**, and sections of IR spectra of 1-MeUH, **1a**, **13**, and **4a** (10 pages); a listing of observed and calculated structure factors (20 pages). Ordering information is given on any current masthead page.

Contribution from the Laboratoire de Chimie Organo-Minérale, UA 422 au CNRS,
Institut de Chimie, 1, rue Blaise Pascal, F-67000 Strasbourg, France

Electrocatalytic Properties of Ni(cyclam)$^{2+}$ and Ni$_2$(biscyclam)$^{4+}$ with Respect to CO_2 and H_2O Reduction

Jean-Paul Collin,* Abdelaziz Jouaiti, and Jean-Pierre Sauvage*

Received December 8, 1987

The electrocatalytic abilities of Ni(cyclam)$^{2+}$ and Ni$_2$(biscyclam)$^{4+}$ have been studied and compared for CO_2 or H_2O reduction. The dimetallic complex is a better electrocatalyst than its monomuclear analogue for evolving H_2 from water. On the other hand, both compounds display analogous properties with respect to CO_2 electroreduction, leading only to C_1 products. In water, CO is the sole reduction product obtained notwithstanding the electrocatalyst used. If low water content DMF is used as a solvent, high faradaic yields of $HCOO^-$ are observed (up to 75%) in addition to CO.

Introduction

Cyclam **1** (1,4,8,11-tetraazacyclotetradecane) displays a very rich coordination chemistry with a large variety of transition metals.[1] In particular, the nickel(II) complex shows a surprising thermodynamic and kinetic stability,[2] which allows its use in a number of catalytic reactions, sometimes under severe conditions. Recent examples include CO_2 electroreduction to CO,[3,4] electrochemical reduction of NO_2^- or NO_3^-,[5] cathodic coupling of alkyl bromides,[6] and epoxidation of olefins.[7] Other related macrocyclic complexes have also been used in electrocatalytic reduction of CO_2.[8] A recent report describes the synthesis of a biscyclam ligand **2** (6,6′-Bi-1,4,8,11-tetraazacyclotetradecane) and its dimetallic complexes[9a] of copper(II) and nickel(II): Cu$_2$(**2**)$^{4+}$, CuNi(**2**)$^{4+}$ and Ni$_2$(**2**)$^{4+}$. Until now the dinickel complex has been used as neither a catalyst nor an electrocatalyst.

This article reports the electrocatalytic properties of Ni$_2$(**2**)$^{4+}$ with respect to CO_2 or H_2O reduction, with particular emphasis on the comparison between the properties of the mononuclear complex Ni(**1**)$^{2+}$ and the dimetallic compound Ni$_2$(**2**)$^{4+}$. Ni$_2$(**2**)$^{4+}$ possesses two coordination sites that might both be close enough to interact simultaneously with small molecules or their reduction products, leading to potentially different reaction pathways than Ni(**1**)$^{2+}$ itself. For instance, the reacting centers of the same molecule could bind to two substrates that would react independently from one another or react in a concerted manner. In the latter case, the reaction products might be different from those obtained by using Ni(**1**)$^{2+}$. As far as CO_2 activation is concerned, an important goal is to favor coupling reactions, leading to C_2 compounds.[10] A general idea is that if two transition-metal centers can be reduced and further react with CO_2 simultaneously, the reduction intermediates obtained from two molecules of CO_2 might form a C–C bond.

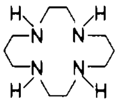

cyclam
1

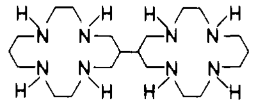

biscyclam
2

Experimental Section

Materials. All products were of reagent grade and were used as received. Acetonitrile (Merck for spectroscopy) and dimethylformamide (DMF) were used without purification. Low water content DMF required for oxalate analysis was obtained by drying commercial grade DMF (Prolabo) overnight over P_2O_5 and distilling under vacuum. The ligand biscyclam (**2**) was obtained by reduction of the bisdioxocyclam[9b] with B_2H_6 as reported previously.[9a] ^1H NMR and mass spectra were as

---

[1] Melson, G. A., Ed. *Coordination Chemistry of Macrocyclic Compounds*; Plenum: New York, 1979.

[2] Busch, D. H. *Acc. Chem.* **1978**, *11*, 392.

[3] Beley, M.; Collin, J. P.; Ruppert, R.; Sauvage, J. P. *J. Chem. Soc., Chem. Commun.* **1984**, 1315.

[4] Beley, M.; Collin, J. P.; Ruppert, R.; Sauvage, J. P. *J. Am. Chem. Soc.* **1986**, *108*, 7461.

[5] Taniguchi, I.; Nakashima, N.; Yasukouchi, K. *J. Chem. Soc., Chem. Commun.* **1986**, 1814. Taniguchi, I.; Nakashima, N.; Matsushita, K.; Yasukouchi, K. *J. Electroanal. Chem. Interfacial Electrochem.* **1987**, *224*, 199.

[6] Becker, J. Y.; Kerr, J. B.; Pletcher, D.; Rosas, R. *J. Electroanal. Chem. Interfacial Electrochem.* **1981**, *117*, 87.

[7] Koola, J. D.; Kochi, J. K. *Inorg. Chem.* **1987**, *26*, 908.

[8] Fisher, B.; Eisenberg, R. *J. Am. Chem. Soc.* **1980**, *102*, 7363.

[9] (a) Fabbrizzi, L.; Montagna, L.; Poggi, A.; Kaden, T. A.; Siegfried, L. C. *Inorg. Chem.* **1986**, *25*, 2671. (b) Fabbrizzi, L.; Forlini, F.; Perotti, A.; Seghi, B. *Inorg. Chem.* **1984**, *23*, 807.

[10] Sneeden, R. P. A. *Comprehensive Organometallic Chemistry*; Wilkinson, G., Stone, F. G. A., Abel, E. W., Eds.; Pergamon: New York, 1982; Vol. 8, Chapter 50.4.

0020-1669/88/1327-1986$01.50/0